IAI Accepts, published online ahead of print on 14 June 2010
Infect. Immun. doi:10.1128/IAI.00111-10




# Immunomodulatory effects of serotype B glucuronoxylomannan from *Cryptococcus gattii* correlate with polysaccharide diameter

Fernanda L. Fonseca[1 Ω], Lilian L. Nohara[2 Ω], Radames J. B. Cordero[3], Susana Frases[5], Arturo Casadevall[3,4], Igor C. Almeida[2 †], Leonardo Nimrichter[1†] and Marcio L. Rodrigues[1*†]

[1]Laboratório de Estudos Integrados em Bioquímica Microbiana, Instituto de Microbiologia Professor Paulo de Góes, Rio de Janeiro, RJ 21941-902, Brazil; [2]Border Biomedical Research Center, Department of Biological Sciences, University of Texas at El Paso, El Paso, TX 79968, USA; Departments of [3]Medicine and [4]Department of Microbiology and Immunology, Albert Einstein College of Medicine, 1300 Morris Park Avenue, Bronx, New York 10461, USA; [5]Laboratório de Biotecnologia, Instituto Nacional de Metrologia, Normalização e Qualidade Industrial, Rio de Janeiro, RJ 25250-020, Brazil.

(*) Corresponding author. Mailing address: Avenida Carlos Chagas Filho 373, CCS, Bloco I. Instituto de Microbiologia, UFRJ. Rio de Janeiro, RJ, Brasil, 21941-902. Phone 55 21 2598 3035; Fax 55 21 2560 8344. Email: marcio@micro.ufrj.br.

Ω FLF and LLN contributed equally to this work.

† ICA, LN and MLR share senior authorship on this article.

**Abstract**

Glucuronoxylomannan (GXM), the major capsular component in the *Cryptococcus* complex, interacts with the immune system in multiple ways, which include activation of Toll-like receptors (TLRs) and modulation of nitric oxide (NO) production by phagocytes. In this study, we analyzed several structural parameters of GXM samples from *C. neoformans* (serotypes A and D) and *C. gattii* (serotypes B and C) and correlated them with the production of NO by phagocytes and activation of TLRs. GXM fractions were differentially recognized by TLR2/1 and TLR2/6 heterodimers expressed on TLR-transfected HEK293A cells. Higher NF-κB luciferase reporter activity induced by GXM was observed in cells expressing TLR2/1 than in cells transfected with TLR2/6 constructs. A serotype B GXM from *C. gattii* was the most effective polysaccharide fraction activating the TLR-mediated response. This serotype B polysaccharide, which was also highly efficient in eliciting the production of NO by macrophages, was similar to the other GXM samples in monosaccharide composition, zeta potential, and electrophoretic mobility. However, immunofluorescence with four different monoclonal antibodies and dynamic light scattering analysis revealed that the serotype B GXM showed particularities in serological reactivity and had the smallest effective diameter among the GXM samples analyzed in this study. Fractionation of additional serotype B GXMs followed by exposure of these fractions to macrophages revealed a correlation between NO production and reduced effective diameters. Our results demonstrate a great functional diversity in GXM samples from different isolates and establish their ability to differentially activate cellular responses. We propose that serologic properties as well as physical chemical parameters such as the diameter of polysaccharide molecules may potentially influence the inflammatory

response against *Cryptococcus* spp. and may contribute to the differences in granulomatous inflammation between cryptococcal species.

## Introduction

*Cryptococcus neoformans* and *C. gattii* are the etiologic agents of the human and animal fungal disease cryptococcosis. Infection is usually acquired by inhalation of environmental basidiospores or desiccated yeasts. Cryptococcal disease in humans can involve every tissue, including cutaneous and pulmonary sites, but the most serious manifestation is central nervous system involvement with meningoencephalitis (43). Despite the similarities of the clinical syndromes in cryptococcosis caused by *C. neoformans* and *C. gattii*, these species differ in the types of host where they cause disease. While *C. neoformans* preferentially causes disease in immunosuppressed patients, *C. gattii*-related disease is relatively common in immunocompetent individuals (33, 43, 48). Mortality rates are still high in different regions of the globe and the current therapeutic options are inefficient (1). No vaccines are available for the prevention of cryptococcosis.

Glucuronoxylomannan (GXM) is the major component of the polysaccharide capsule, which is the main virulence factor of *Cryptococcus* species (30). GXM is an anionic polysaccharide consisting of a α1-3 linked mannan that is *O*-acetylated at the carbon 6 of some of the mannosyl units and substituted with β1,2 glucuronyl and β1,2 / β1,4 xylosyl residues (9). The polysaccharide is a capsular component of *Cryptococcus* species that is also abundant in its soluble form in culture fluids and infected tissues (31). Secreted and surface-associated GXM are believed to modulate the immune response during cryptococcosis through multiple mechanisms (35). In addition, administration of monoclonal antibodies against GXM can modify the course of experimental cryptococcosis by prolonging host survival (3). Four serotypes of GXM (A–D) have been defined by serological reactions. This classification divides

74 pathogenic *Cryptococcus* species with specific serotypes, such that *C. gattii* consists
75 of serotypes B and C isolates while *C. neoformans* varieties *grubii* and *neoformans*
76 correspond to serotypes A and D, respectively (23, 43). Most studies on the
77 immunological functions of GXM have focused on the polysaccharide fractions from
78 serotype A *C. neoformans* isolates. Although it is generally assumed that the
79 immunological properties observed for the serotype A polysaccharide are applicable
80 to the other serological groups, this common assumption may not be correct given
81 major structural differences among the four major serotypes.

82 The ability of GXM to activate the innate immune response was previously
83 reported in several studies (34, 46, 52, 53). Serotype A GXM was reported to
84 modulate the production of nitric oxide (NO) by phagocytes (5). In addition, GXM
85 activates Toll-like receptor (TLR) 4-mediated intracellular signaling (46), but the
86 contribution of this event to the global innate response against *C. neoformans*
87 infections is uncertain (2, 39). GXM can also interact with TLR2 (46), which is
88 believed to influence the response to cryptococcal infection (53). TLR2 recognizes a
89 diverse set of pathogen-associated molecular patterns, which requires
90 heterodimerization with TLR 1 or 6 (14, 17, 22, 29, 50). The roles of TLR1 or TLR6
91 in the recognition of GXM by TLR2 have not been investigated yet.

92 In this study, we correlated the structural and physical chemical properties of
93 five GXM samples with their ability to stimulate NO production by macrophages and
94 to activate nuclear factor κB (NF-κB) in cells expressing either TLR2/TLR1 or
95 TLR2/TLR6. Our results demonstrate that a serotype B GXM sample is particularly
96 efficient in activating these cellular responses. These immunomodulatory properties
97 correlate with specific serologic properties and to a reduced diameter of
98 polysaccharide molecules.

## Material and methods

**Fungal strains.** Cryptococcal isolates used in this study were selected from the culture collection available in our laboratory. Strains that had previously been more extensively characterized according to their phenotypic characteristics, such as capsule expression, serotype, growth rate and biochemical properties (6), were used for structural and immunological assays. These samples included strains $T_1$444, HEC3393 (serotype A, clinical isolates) and ATCC28938 (serotype D, obtained from the American Type Culture Collection, Manassas, VA) of *C. neoformans* and CN23/10.993 (serotype B, environmental isolate) and HEC40143 (serotype C, environmental isolate) strains of *C. gattii*. Additional serotype B strains were included in this study based on the results obtained during structural/immunological investigations. These isolates comprised the well characterized strain R265 (19) and strain ATCC56990 (American Type Culture Collection). Stock cultures were maintained in Sabouraud dextrose agar under mineral oil and kept at 4°C.

**GXM purification.** GXM was isolated as previously described by our group (40). Briefly, *C. neoformans* and *C. gattii* cells (4 x $10^9$ cells) were suspended in 100 ml of a minimal medium composed of glucose (15 mM), $MgSO_4$ (10 mM), $KH_2PO_4$ (29.4 mM), glycine (13 mM), and thiamine-HCl (3 µM); pH 5.5. For all experiments we used LPS-free water and glassware. This suspension was then transferred to a 1000-ml Erlenmeyer flask and supplemented with 300 ml of the same medium. Fungal cells were cultivated for four days at room temperature, with shaking and separated from culture supernatants by centrifugation at 4,000 *g* (15 min, 4°C). The supernatant fluids were collected and again centrifuged at 15,000 *g* (15 min, 4°C), to remove smaller

124 debris. The pellets were discarded and the resulting supernatant was concentrated
125 approximately 20-fold using an Amicon (Millipore, Danvers, MA) ultrafiltration cell
126 (cutoff = 100 kDa, total capacity of 200 ml) with stirring and Biomax
127 polyethersulfone ultrafiltration discs (63.5 mm). Nitrogen ($N_2$) stream was used as the
128 pressure gas. After supernatant concentration, the viscous layer formed was collected
129 with a cell scraper and transferred to graduated plastic tubes for measurement of gel
130 volumes. The procedure was repeated at least three times to ascertain average
131 volumes. Alternatively, the supernatant fraction passed through the 100 kDa
132 membrane was again concentrated using a 10 kDa filtration disc. The viscous layer
133 was again collected and used for structural and functional determinations.
134
135 **ELISA for GXM quantification**. The concentration of GXM in supernatants and
136 concentrated films was determined by capture ELISA, as previously described (4).
137 Briefly, 96-well polystyrene plates were coated with a goat anti-mouse IgM. After
138 removal of unbound antibodies, a solution of mAb 12A1, an IgM mAb with
139 specificity for GXM, was added to the plate, and this step was followed by blocking
140 with 1% bovine serum albumin. Supernatants in different dilutions or purified GXM
141 were added to the wells and the plates were incubated for 1 h at 37°C. The plates were
142 then washed five times with a solution of tris-buffered saline (TBS) supplemented
143 with 0.1% Tween 20, followed by incubation with mAb 18B7 for 1 h. This antibody,
144 is a well characterized IgG1 that protects mice against lethal challenges with *C.*
145 *neoformans* and binds to an epitope found in GXM from serotypes A, B, C and D (3).
146 The plate was again washed and incubated with an alkaline phosphatase-conjugated
147 goat anti-mouse IgG1 for 1 h. Reactions were developed after the addition of *p*-
148 nitrophenyl phosphate disodium hexahydrate, followed by measuring absorbance at

405 nm with a microplate reader (TP-reader, Thermo Plate). The antibodies used in this assay were used at 1 μg/ml.

**Monosaccharide analysis**. Carbohydrate composition analysis was performed by gas chromatography-mass spectrometry (GC-MS) analysis of the per-*O*-trimethylsilyl (TMS) derivatized monosaccharides from the polysaccharide films, according to the methodology described by Merkle and Poppe (32). Methyl glycosides were first prepared from the dry sample (0.3 mg) by methanolysis in methanol-1 M HCl at 80°C (18-22 h). The sample was then per-*O*-trimethylsilylated by treatment with Tri-Sil (Pierce) at 80°C (0.5 h). GC-MS analysis of the per-*O*-TMS derivatives was performed on an HP 5890 gas-chromatographer interfaced to a 5970 MSD mass spectrometer, using a Supelco DB-1 fused-silica capillary column (30 m x 0.25 mm ID). Carbohydrate standards used were arabinose, rhamnose, fucose, xylose, glucuronic acid, galacturonic acid, mannose, galactose, glucose, mannitol, dulcitol, and sorbitol.

**Transient transfection with TLRs.** TLR constructs (16) as well as the β-actin *Renilla* luciferase (49) and the reporter ELAM-1-firefly luciferase (45) constructs were kindly provided by Dr. Richard Darveau (University of Washington, Seattle, WA). All plasmids used in the transfections were purified using the EndoFree Plasmid Purification Maxi Kit (Qiagen, Valencia, CA) following the manufacturer's instructions. HEK293A cells (ATCC, Manassas, VA) were cultured in high glucose Dulbecco's Modified Eagle Medium (DMEM) (Sigma-Aldrich, St. Louis, MO) supplemented with 10% heat-inactivated fetal bovine serum (FBS) (HyClone, Logan, UT) and the confluent monolayer harvested by treatment with trypsin/EDTA (Sigma-

Aldrich, St. Louis, MO). Cells were seeded in 12-well plates the day before transfection. HEK293A cells were transiently cotransfected with plasmids encoding mouse TLR2 and TLR1 or TLR2 and TLR6 together with the reporter construct ELAM-1-firefly luciferase and β-actin *Renilla* luciferase using Lipofectamine 2000 (Invitrogen, Carlsbad, CA) according to the manufacturer's recommendations. Total DNA per well was normalized to 2 µg by adding empty vector. On the following day, the transfected cells were plated in 96-well plates.

**Luciferase reporter assays for NF-κB activation.** Forty-eight hours after transfection, cells were stimulated with purified GXM (1-100 µg/ml) for 4 h in DMEM containing 10% FBS. Controls for TLR activation included stimulation of cells with ultra pure lipopolysaccharide (LPS) from *E. coli* 0111:B4 strain (Invivogen, San Diego, CA), $Pam_3Cys$-SKKKK (P3C) or FSL-1 (EMC Microcollections, Tübingen, Germany). Then, cells were washed once in phosphate buffered saline (PBS) and lysed in Passive Lysis Buffer (Promega, Madison, WI). The luciferase activity was measured using the Dual-Luciferase Reporter Assay System (Promega, Madison, WI) according to the manufacturer's instructions. The relative light-units (RLU) were quantitated using a Luminoskan luminometer. NF-κB activation is expressed as the ratio of NF-κB-dependent firefly luciferase activity to β-actin-dependent *Renilla* luciferase activity (16). The results are shown as the means and standard deviations of values for triplicate wells.

**Nitric oxide production by phagocytes**. The murine macrophage-like cell line RAW 264.7 (ATCC) was cultivated under LPS-free conditions in complete DMEM supplemented with10% fetal calf serum (FCS), 2 mM L-glutamine, 1 mM sodium

pyruvate, 10 mg ml/ml gentamicin, MEM non-essential amino acids (Gibco-Invitrogen 11360), 10 mM HEPES and 50 mM 2- beta-mercaptoethanol, at 37 °C in a 7.5% $CO_2$ atmosphere. Murine cells were washed twice in serum-free DMEM and incubated in fresh medium supplemented with varying concentrations of GXM (1-100 μg/ml) for 16 h at 37°C (7.5% $CO_2$ atmosphere). As a positive control, macrophages were stimulated with 1 μg/ml LPS. Supernatants were then collected and assayed for NO production by the method of Griess (15). Negative controls consisted of supernatants of RAW cells cultivated in medium containing no GXM. All experiments were performed in triplicate sets.

**Immunofluorescence for GXM detection**. Antibodies to GXM used in this assay included immunoglobulins (Ig) G and M. MAbs 12A1 and 13F1 are two clonally related IgMs that differ in fine specificity and protective efficacy (37, 38). MAb 12A1 is protective and produces annular immunofluorescence (IF) on serotype D *C. neoformans,* while MAb 13F1 is not protective and produces punctate IF. MAb 2D10 (IgM) is also protective in a murine model of cryptococcosis. This antibody reacts with epitopes found through the cell wall and capsule of a serotype D strain of *C. neoformans* (13). MAb 18B7 is a protective IgG1 that has been tested as a therapeutic antibody in animals and humans (3, 24). This antibody reacts with all GXM serotypes. *C. neoformans* cells ($10^6$) were fixed with 4% paraformaldehyde. The cells were further blocked for 1 h in PBS-BSA and incubated with the mAbs described above (1 μg / ml) for 1 h at room temperature, followed by fluorescein isothiocyanate (FITC) labeled goat anti-mouse (IgG or IgM) antibodies (Sigma). Yeast cells were finally observed with an Axioplan 2 (Zeiss, Germany) fluorescence microscope. Images were acquired using a Color View SX digital camera and processed with the software

system analySIS (Soft Image System). In control conditions mAbs were replaced by isotype-matched irrelevant antibodies. Exposure times were similar for all conditions.

**Biophysical studies.** Particle size and negative charge of GXM samples were inferred from dynamic light scattering and zeta potential (ζ) determinations, respectively, following the methods described by Frases and colleagues (11, 12). For ζ determination, GXM solutions were adjusted to 1 mg/ml in water and analyzed in a Zeta potential analyzer (ZetaPlus, Brookhaven Instruments Corp., Holtsville, NY). Final values were obtained from the equation $\zeta = (4\pi\eta m)/D$, where $D$ is the dielectric constant of the medium, η is the viscosity, and $m$ is the electrophoretic mobility of the particle. For determination of GXM effective diameter, polysaccharide solutions were prepared as described above and measured by Quasi elastic light scattering in a 90Plus/BI-MAS Multi Angle Particle Sizing analyzer (Brookhaven Instruments Corp., Holtsville, NY). Particle size values were calculated as described recently (12). Multimodal size distribution analysis of polysaccharides was calculated from the values of intensity weighted sizes obtained from the non-negatively constrained least squared (NNLS) algorithm.

**Statistics.** The existence of significant differences between the different systems analyzed in this study was ascertained using multiple statistical tests. Efficacy of TLR-mediated NF-κB activation, NO production and correlation tests and biophysical tests were statistically evaluated using Student's *t* test when two different groups were compared, and analysis of variance for comparison of several groups. Statistical tests were performed with GraphPad Prism (version 5.0).

## Results

**GXM from all strains manifest aggregation characteristics**. GXM aggregation resulting in the production of purified gels of native polysaccharide was previously demonstrated for a serotype D strain of *C. neoformans* (11, 40). However, it was unclear whether formation of the viscous polysaccharide films was a strain-specific phenomenon or a general property of cryptococcal strains. Therefore, we evaluated the ability of polysaccharide from two *C. neoformans* var. *grubii* and *C. gattii* (serotypes B and C) to form gels after concentration by ultrafiltration.

Supernatants were obtained from 400 ml-cultures containing an initial inoculum of $4 \times 10^9$ cells. The final number of cells in each culture varied according to the growth rate of each strain (not shown). Supernatant concentration by ultrafiltration led to the deposition of viscous films on filters for all isolates tested. The volumes of the films were normalized to the final cell numbers of each culture. This procedure was repeated at least three times for each strain and different average values of polysaccharide volume were generated (Figure 1A). Next, we analyzed the ability of each isolate to produce extracellular GXM, normalizing the polysaccharide concentration found by ELISA to the final cell number in the culture. The profile of GXM production by each strain, determined by ELISA (Figure 1B), resembled very closely that observed for gel formation in the corresponding supernatant. In fact, GXM concentrations in supernatants and gel formation were correlated ($R^2 = 0.7390$; $P = 0.0014$), as demonstrated in Figure 1C.

The sugar composition of each polysaccharide fraction was analyzed by GC-MS (Figure 1D). After methanolysis of the polysaccharides and per-*O*-trimethylsilylation of the corresponding products, the resulting monosaccharides were initially identified by their retention times relative to standards, followed by structural

authentication using MS/MS (not shown). All polysaccharide samples tested revealed xylose, mannose and glucuronic acid as major constituents, consistent with the three sugar components of GXM. As previously reported (10, 11), galactose was a trace component of all samples (data not shown). The levels of each GXM building unit varied in polysaccharides from each isolate (Figure 1D), as normally observed during analysis of different GXM samples. Strains HEC3393 (serotype A) and HEC40143 (serotype C) contained particularly high proportions of xylose, while strains $T_1444$ (serotype A), CN23/10993 (serotype B) and ATCC28938 (serotype D) had mannose as their major monosaccharide constituent.

**NF-κB activation in cells expressing TLR2/1 or TLR2/6 heterodimer in response to GXM**. HEK293A cells expressing either TLR2/1 or TLR2/6 were stimulated with the control molecules LPS, P3C, and FSL-1 or with five different GXM fractions obtained from *C. neoformans* and *C. gattii* (Figure 2). Transfected cells showed efficient NF-κB activation in response to the synthetic triacylated lipopeptide P3C and to the synthetic diacylated lipopeptide FSL-1, which were used as positive controls for TLR2/1 and TLR2/6 activation, respectively (21). As expected, TLR2/6- or TLR2/1-transfected cells responded very poorly to LPS, the classic TLR4 ligand (18). Also, HEK293A cells transfected with the reporter construct and plasmids containing no TLR-coding sequences (vector) were unresponsive in all cases. All polysaccharide samples induced a dose-dependent activation of NF-κB (Figure 2). NF-κB activation by GXM was always more efficient in cells transfected with the TLR2/1 constructs. Translocation of NF-κB in GXM-treated cells was also more efficient in cells expressing TLR2/1 than in cells transfected with plasmids coding for TLR4/CD14

(data not shown), which were initially described as the receptors involved in GXM-mediated TLR activation (46).

A comparative analysis of the ability of each GXM sample to activate TLR-mediated cellular responses revealed unexpected differences. Although all polysaccharide fractions had the capacity to activate NF-κB in either TLR2/1- or TLR2/6-expressing cells at the concentration of 100 μg/ml, a *C. gattii* polysaccharide sample (serotype B) was significantly more efficient at activating NF-κB than all others ($P<0.0001$), with strong signals apparent at 1 and 10 μg/ml (Figure 3). At 1 μg/ml, NF-κB activation mediated by the serotype B GXM was at least 10-fold more efficient than all others for TLR2/1-expressing cells and 6-fold higher for TLR2/6-expressing cells. At 10 μg/ml, the serotype B sample was approximately 2-fold and 4-fold more effective than the other samples in TLR2/1- and TLR2/6-expressing cells, respectively.

**NO production in response to GXM stimulation.** The GXM samples used for TLR activation were also tested for their ability to stimulate the production of NO by macrophage-like cells. Exposure of RAW 264.7 cells to GXM from *C. neoformans* cultures resulted in the production of NO at the background level (Figure 4). Treatment of the phagocytes with *C. gattii* GXM, however, resulted in a dose-dependent production of NO. As observed in TLR-based assays, the GXM sample from strain CN23/10993 was the most effective polysaccharide fraction in eliciting NO production.

**Structural and serological properties of GXM from *C. neoformans* and *C. gattii*.** The differences in the TLR-activating ability of the various GXM samples led us to

investigate the antigenic and physical properties of this polysaccharide set in more detail. The differences in the monosaccharide composition in each sample were not correlated with the ability of GXM to activate cellular responses, since polysaccharide fractions with very similar compositions (strains CN23/10993 and ATCC28938) manifested different efficacies in NO and TLR2/1- and TLR2/6-mediated NF-κB activation (Figures 1-4).

The negative charge of GXM is an important determinant of function for the capsular polysaccharide in *C. neoformans* (40, 41). Consequently, we determined the zeta potential of the GXM from each *C. neoformans* and *C. gattii* isolates and these were similar (Table 1). The electrophoretic mobility of each GXM preparation was also similar and strictly correlated with zeta potential values ($r^2 = 0.9992$, $P<0.0001$). These results therefore suggested that polysaccharide charge did not affect activation of NO production and TLR-mediated cellular responses by GXM.

Differences in GXM structure and functions can correlate with reactivity with monoclonal antibodies (42), which led us to evaluate whether the functional discrepancies observed in Figures 2-4 would be related with specific serological patterns (Figure 5). Cells from each of the five *C. neoformans* strains were similarly recognized by mAb 18B7, as demonstrated by immunofluorescence analysis. For all strains, there was comparable intensity and the binding pattern was annular. MAbs 2D10, 12A1 and 13F1 produced punctate patterns of reactivity with similar intensities after incubation with strains $T_1$444, HEC3393, HEC40143 and ATCC28938. When strain CN23/10993 was used, however, very strong serologic reactions were observed with mAb 12A1. In contrast, these cells were not recognized by mAb 13F1.

**GXM effective diameter**. Epitope accessibility in GXM may vary according to the diameter of the molecule (11). In addition, polysaccharide size is a parameter known to influence activation of TLR2-mediated innate responses (26). We therefore investigated the relationship between NF-κB activation and GXM effective diameter as measured by dynamic light scattering (Figure 6). The polysaccharide molecules with the largest diameters came from isolates $T_1$444 and ATCC28938 (serotypes A and D, respectively). GXM from strains HEC3393 and HEC40143 (serotypes A and C, respectively) showed smaller diameter values, which were still higher than that obtained for the polysaccharide isolated from strain CN23/10993 (serotype B). All strains produced polysaccharides with diameters higher than 2 μm, except for strain CN23/10993. Effective diameter determination in ten different analyses showed that GXM fractions from the CN23/10993 isolate were significantly shorter ($P$<0.0001) than any other polysaccharide. Therefore, the GXM sample containing molecules of the smallest diameter was the most potent one in activating the cellular responses in this study.

**Smaller GXM fractions from serotype B *C. gattii* strains are more effective in eliciting NO production**. In an attempt to establish a correlation between the effective diameter of GXM samples and their ability to stimulate cellular responses, we fractionated culture supernatants of different cryptococcal isolates. GXM samples were isolated from different strains, including: i) $T_1$444, due to its ability to abundantly produce extracellular polysaccharides with high-diameter (Figures 1 and 6), and ii) CN23/10993, which was selected based on its ability to produce GXM with apparently higher immunogenicity (Figures 2-4). Two additional serotype B GXMs, from strains R265 and ATCC56990, were included in this assay for comparative

372 purposes. GXM fractions with molecular masses higher than 100 kDa and in the range
373 of 10-100 kDa were obtained by supernatant filtration and the prototype assay used to
374 analyze the relationship between the size of GXM samples and their ability to
375 stimulate cellular responses was NO production by macrophages, since it includes
376 straightforward procedures and simple data interpretation.

377 Fractionation of the $T_1$444 supernatant revealed that the high molecular mass
378 sample (>100 kDa) induced NO production by the phagocytes more efficiently ($P <$
379 0.001) than the polysaccharide fraction in the 10-100 kDa mass range (Figure 7A). An
380 opposite pattern was observed for the *C. gattii* samples. All GXM fractions of lower
381 molecular masses were significantly more effective in stimulating the production of
382 NO than the high molecular weight polysaccharides ($P < 0.0001$ for all samples).
383 Again, GXM fractions from strain CN23/10993 were the most effective samples
384 inducing NO production. Measurements of polysaccharide effective diameter in these
385 fractions were performed by dynamic light scattering, which confirmed that samples
386 with higher molecular masses consisted of molecules of increased dimensions (Figure
387 7B). Analysis of serotype B GXM samples (strains CN23/10993, R265 and
388 ATCC56990) in the 10-100 kDa molecular mass range revealed a direct correlation
389 between their ability to induce NO and reduced effective diameters (Figure 7C).
390
391
392

## Discussion

Recent studies indicate that the structure of GXM and, consequently, its biological functions vary according to parameters that include molecular mass and effective diameter (11, 12, 40). The functional diversity in cryptococcal polysaccharides is not exclusive to GXM. In fact, it has been recently described that galactoxylomannan (GalXM) samples from *C. neoformans* are structurally and antigenically variable (8). Therefore, establishing general functions for cryptococcal polysaccharides is complex, since very different characteristics of supposedly similar samples have been repeatedly observed in independent studies (8, 11, 40), that presumably reflect differences in polysaccharide structure. GXM, for instance, has been classically defined as deleterious to the immune system (51), although it can also activate the host defense (46).

Fungal polysaccharides are potential candidates to activate TLR2-mediated cellular responses. In *Histoplasma capsulatum*, $\beta$-glucan-induced formation of lipid bodies, which are multifunctional organelles with critical roles in inflammation, was inhibited in TLR2-deficient mice (47). Chitin, a cell wall structural polysaccharide, has been consistently characterized as a stimulator of TLR2-dependent production of IL-17 by macrophages, resulting in the induction of acute inflammation (7).

The ability of *C. neoformans* GXM to activate TLR-mediated innate responses was demonstrated in a number of previous studies (2, 27, 28, 36, 39, 46, 53), but comparable studies have not been carried out for *C. gattii* polysaccharides. TLRs and the CD14 receptor function as pattern recognition receptors for GXM (27, 28, 36, 44, 46, 53). The binding of GXM to TLR4 was reported to result in translocation of NF-κB to the nucleus in an incomplete process that does not induce activation of mitogen-activated protein kinase pathways or release of TNF-α (46). TLR4 was also

implicated as a receptor involved in cellular uptake (34), and tissue distribution (52) of GXM. However, the roles of TLR2 and other TLRs in the immune response to GXM remain poorly understood. In the present study, we determined that the hydrodynamic size of GXM fractions is correlated with their ability to stimulate NO production by macrophages and to activate NF-κB in a TLR2-dependent manner. In fact, all GXM fractions stimulated activation of NF-κB in HEK293A cells transiently transfected with TLR2 and TLR6, or TLR2 and TLR1 constructs. This response was always more intense in cells expressing the TLR2/1 association than in those expressing the TLR2/6 construct. In all systems, the highest levels of NF-κB activation were obtained when transfected HEK293A cells were exposed to a serotype B GXM from the *C. gattii* strain.

To understand the structural characteristics responsible for NO and TLR activation we evaluated several GXM parameters. The ability of GXM to induce NO production and the TLR-mediated response in transfected HEK293A cells was not an intra-species property nor depended on sugar composition, so other parameters were evaluated. Differences in antibody reactivity can imply differences in GXM structure (11), which also denote functional specificity (20). In this study we found that the serologic characteristics revealed by the binding of mAbs were similar in all strains, except for the *C. gattii* strain CN23/10993. Those cells showed strong reactivity with the protective IgM 12A1, but did not react with the clonally-related, non-protective mAb 13F1. This observation is consistent and reflective of the fact that mAbs 12A1 and 13F1 bind to different epitopes. In a recent study, it has been suggested that antibody reactivity is influenced by the diameter of GXM (10), which led us to the inference that the effective diameter of the polysaccharide samples used in this study could also be related to the functionality of GXM.

Immunological studies with chitin have shown that large polysaccharide polymers are biologically inert, while their fragments are efficient regulators of TLR2-mediated innate immune responses (7, 25, 26). Human cryptococcosis caused by *C. gattii* is known to produce strong inflammatory responses in the lung, whereas the *C. neoformans* varieties often trigger little or no inflammation (49). Consequently, the result that serotype B GXMs were more potent activators of cellular responses raises the tantalizing possibility that a correlation might exist between activation of host cells and the type of granulomatous response made. In our model, the most effective GXM sample in activating cellular responses had the smallest effective diameter, a result that echoed previous findings with chitin (7, 25, 26). Using the model of NO production by macrophages after exposure to the serotype B GXM, we observed that polysaccharides with reduced dimensions induced a stronger cellular response, a property that was exclusive to serotype B GXM samples. NO production by macrophages is involved in both antimicrobial responses and mediation of inflammation, illustrating the complex effects of the GXM on host immune function. Given that our studies compared GXM preparations standardized by mass/volume and that smaller fibers have lower molecular masses, it is possible that the effects measured here reflect differences in the molarity of the GXM. Nevertheless, we urge caution in attributing these effects to simple differences in molarity since interactions between polysaccharides and their receptors are likely to involve repeating structural motifs in polysaccharide molecules such that avidity considerations could be dominant. Furthermore, we note that immunological studies routinely measure effects using polysaccharide concentrations standardized by mass/volume and consequently this approach is experimentally relevant, especially for literature comparisons.

The cryptococcal capsule enlarges during infection, which is essential for virulence (54). A linear correlation between the effective diameter of GXM and microscopic capsular diameter was recently demonstrated (12), suggesting that the synthesis of high-diameter polysaccharides is essential for capsule enlargement. In our model, strain CN23/10993 produced GXM molecules with the lowest values of effective diameter and had the smallest capsular dimension (data not shown). The combination of the ability of GXM to modulate cellular responses and the capacity of *C. neoformans* to produce large GXMs and capsules may have a direct impact on fungal virulence. *C. neoformans* isolates producing large GXM molecules would be more efficient in producing capsules with increased dimensions, which is generally associated with pathogenic potential (54). On the other hand, isolates producing smaller GXMs, according to our current results, would manifest a potentially enhanced ability to activate some mechanisms of the immune response. Considering that the cryptococcal capsule also protects the fungus against a number of antifungal mechanisms of the host, a combination of smaller GXMs and formation of a capsular network with reduced dimensions would favor the host defense by multiple mechanisms. We therefore suggest that synthesis of capsular structures with reduced dimensions could have protean effects on the pathogenic capacity of cryptococcal strains ranging from increased susceptibility to oxidative fluxes and phagocytosis, to producing molecules with an enhanced ability to activate host defenses. These observations suggest a mechanistic explanation for the consistent observation that strains with small capsules elicit more inflammation than those with large capsules (43). Furthermore, the higher NO-inducing activity associated with *C. gattii* polysaccharides, which correlates with smaller GXM diameters, suggests an

explanation for the consistent observation of stronger granulomatous responses in cryptococcosis caused by this species (33, 43, 48).

**Acknowledgements**.

MLR and LN are supported by grants from Coordenação de Aperfeiçoamento de Pessoal de Nível Superior (CAPES, Brazil), Conselho Nacional de Desenvolvimento Científico e Tecnológico (CNPq, Brazil), Fundação de Amparo a Pesquisa do Estado de São Paulo (FAPESP, Brazil) and Fundação de Amparo a Pesquisa do Estado do Rio de Janeiro (FAPERJ, Brazil). AC is supported by NIH grants AI033142, AI033774, AI052733, and HL059842. ICA is supported by NIH/NCRR grant 5G12RR008124-16A1. LLN is partially supported by the Cotton Memorial Scholarship (UTEP), Good Neighbor Scholarship (UTEP), and Florence Terry Griswold Scholarship-I (PARTT). RJBC is supported by the Training Program in Cellular and Molecular Biology and Genetics, T32 GM007491. Carbohydrate analyses were performed at the Complex Carbohydrate Research Center, University of Georgia-Athens, which is supported in part by the Department of Energy-funded (DE-FG-9-93ER-20097) Center for Plant and Microbial Complex Carbohydrates. TLR experiments were partly carried out at the Biomolecule Analysis (BACF) and the Cell Culture and High Throughput Screening Core Facilities, the Border Biomedical Research Center (BBRC), UTEP, supported by NIH/NCRR grants 5G12RR008124-16A1 and 3G12RR008124-16A1S1 (BACF). We thank Jorge José Jó B. Ferreira and Rosana Puccia for helpful discussions and Natalia Freire for help with GXM fractionation. We are also indebted to Drs Sonia Rozental and Marilene Vainstein for the gifts of strains ATCC56990 and R265.

518 **Figures**

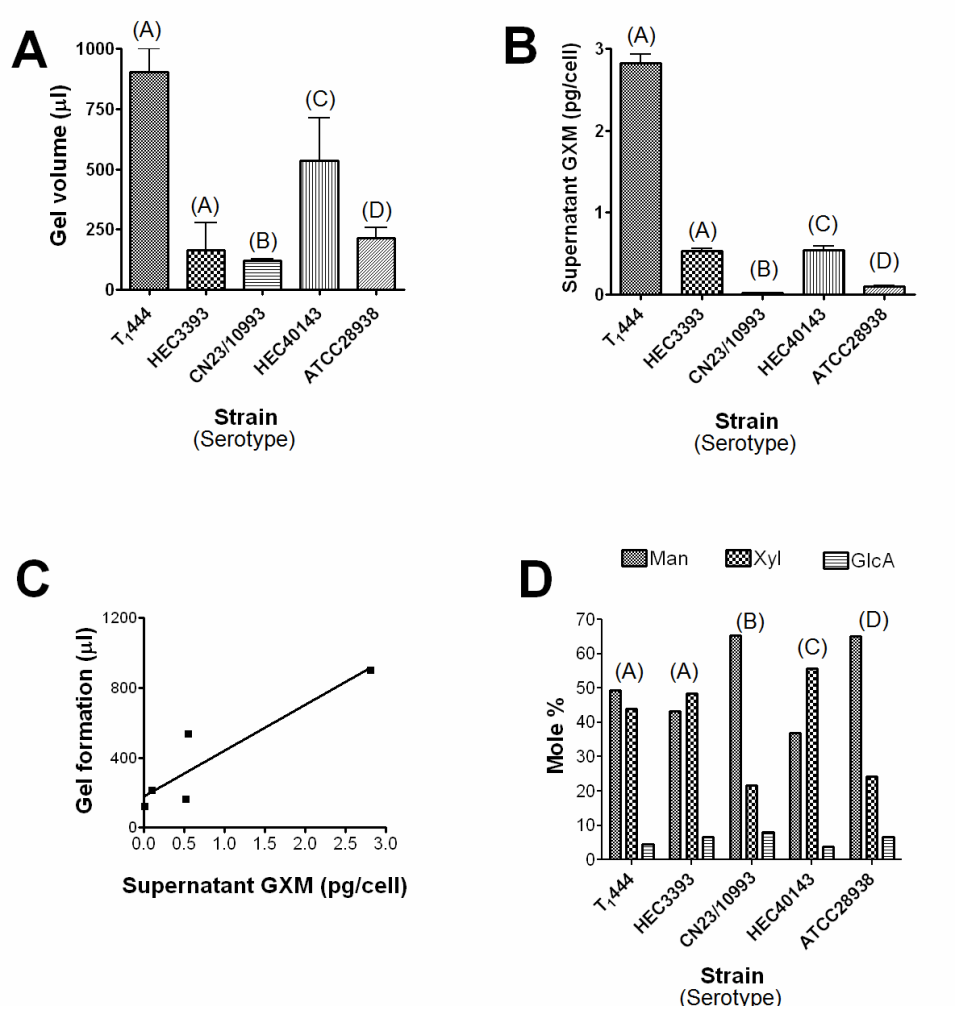


519

520 **Figure 1. Quantitative and structural analyses of GXMs from five *Cryptococcus***
521 **isolates.** GXM was isolated by formation of polysaccharide gels after concentration of
522 culture supernatants of five different isolates of *C. neoformans* and *C. gattii*. The
523 volume of gel formation in normalized cultures (A) apparently correlates with the
524 ability of each strain to produce and secrete GXM to the extracellular medium (B).
525 Results are expressed as means ± standard deviations of three different experiments.
526 Correlation properties are shown in C. D. Monosaccharide composition of
527 polysaccharides obtained from the five different isolates of *C. neoformans* and *C.*

528 *gattii*. Monosaccharides were identified by GC-MS; the relative amount of each sugar
529 residue in the polysaccharides is shown as molar percentage. Serotypes are indicated
530 for each strain.
531

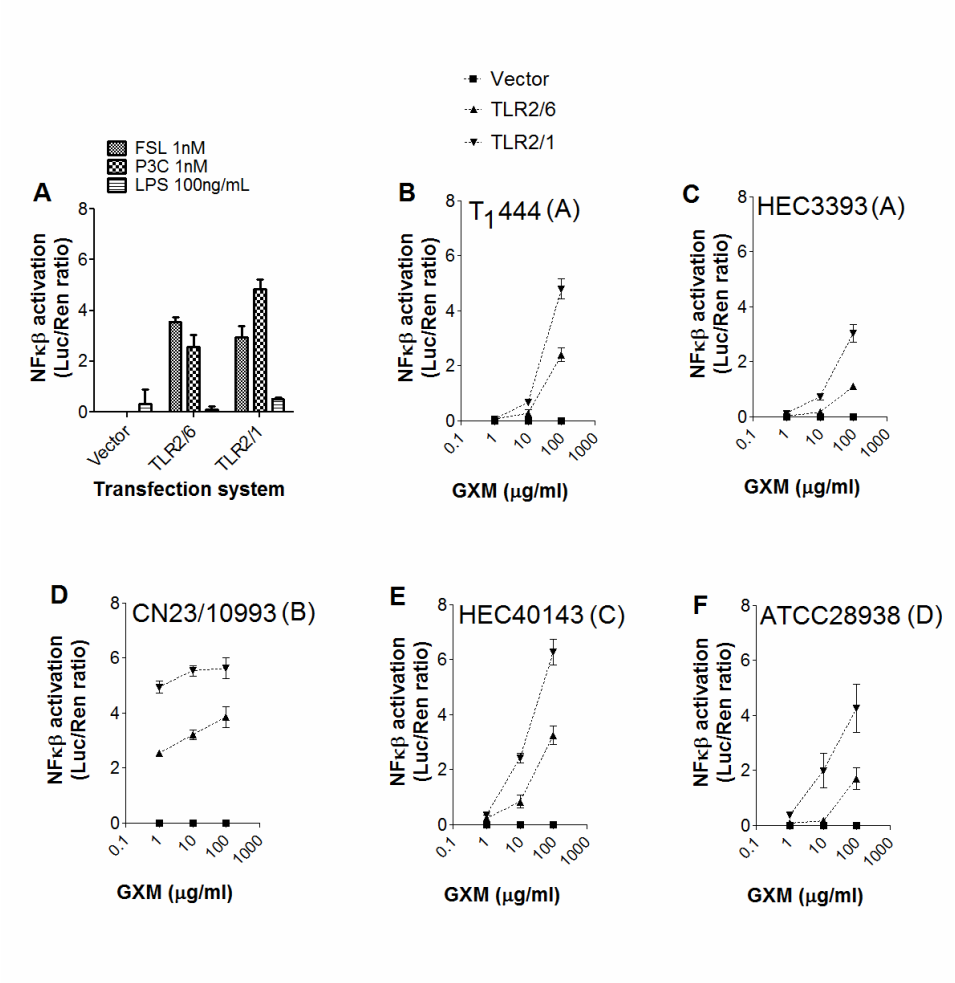


532

533

534 **Figure 2. NF-κB activation in cells expressing TLRs by GXM**. A. Control systems.

535 $Pam_3CSK_4$ ($P_3C$) and FSL-1, but not LPS, activated NF-κB nuclear translocation in

536 cells expressing either TLR2/1 or TLR2/6, as expected. Transfection of HEK293A

537 cells with a plasmid containing no TLR-coding sequences (vector) resulted in

538 unresponsiveness. B-E. Stimulation of HEK293A cells expressing TLR2/1 (inverted

539 triangles) or TLR2/6 (triangles) to GXM samples resulted in dose-dependent NF-κB

540 activation. *Cryptococcus* strains and serotypes from which each GXM sample was

541 isolated are indicated in each panel.

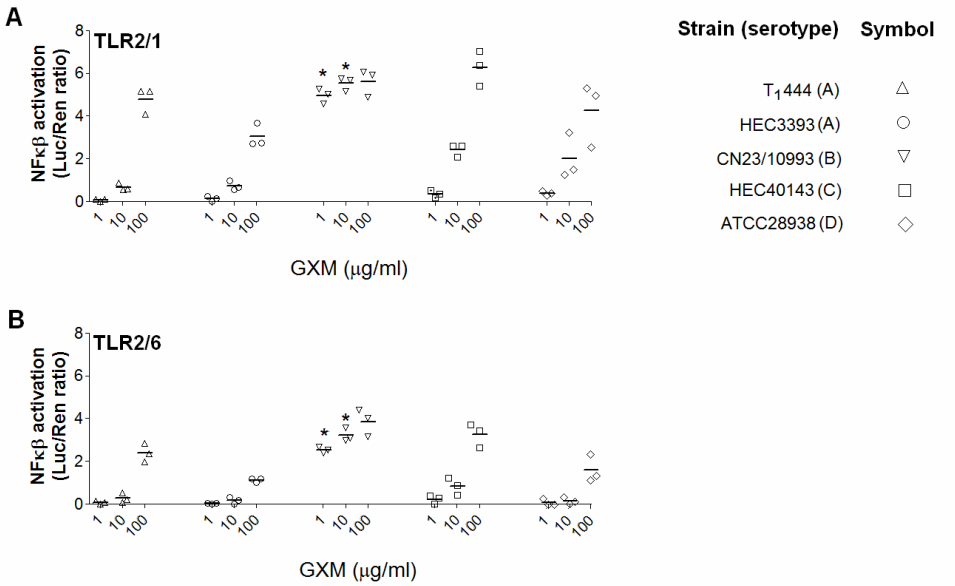


**Figure 3. Comparative analysis of the efficacy of GXM samples in the activation of TLR-mediated NF-κB nuclear translocation**. Treatment of HEK293A cells expressing either TLR2/1 (A) or TLR2/6 (B) with GXM revealed that polysaccharide fractions from strain CN23/10993 were significantly more efficient than all others ($P$<0.0001) at 1 and 10 μg/ml (asterisks). No significant differences were observed at a higher concentration (100 μg/ml). Strains $T_1$444, HEC3393, HEC40143 and ATCC28938 manifested similar efficacies in activating NF-κB nuclear translocation. Strain serotypes are indicated.

555

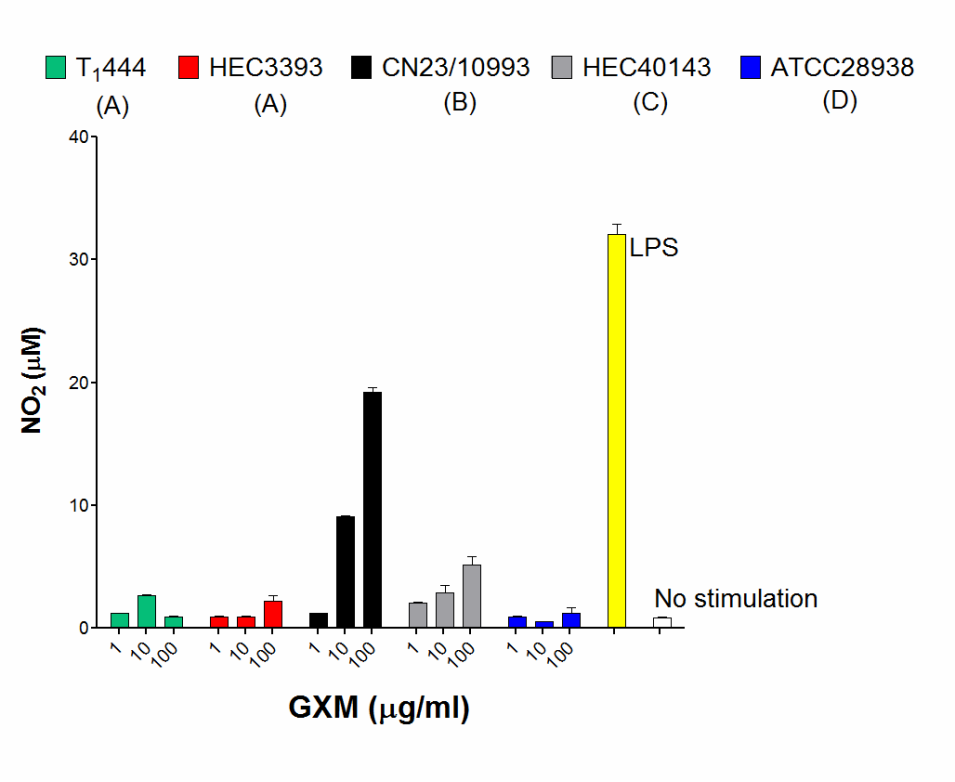


556

557 **Figure 4. Comparative analysis of the efficacy of GXM samples in the induction**
558 **of NO production by macrophages**. Polysaccharide fractions from strain
559 CN23/10993 were significantly more efficient in induction of NO production than all
560 others ($P$<0.0001) at 1, 10 and 100 μg/ml. LPS was used as positive control of NO
561 production by macrophage-like cells; incubation of the phagocytes in the medium
562 alone (no stimulation) was the negative control. Serotypes are indicated for each
563 strain.

564

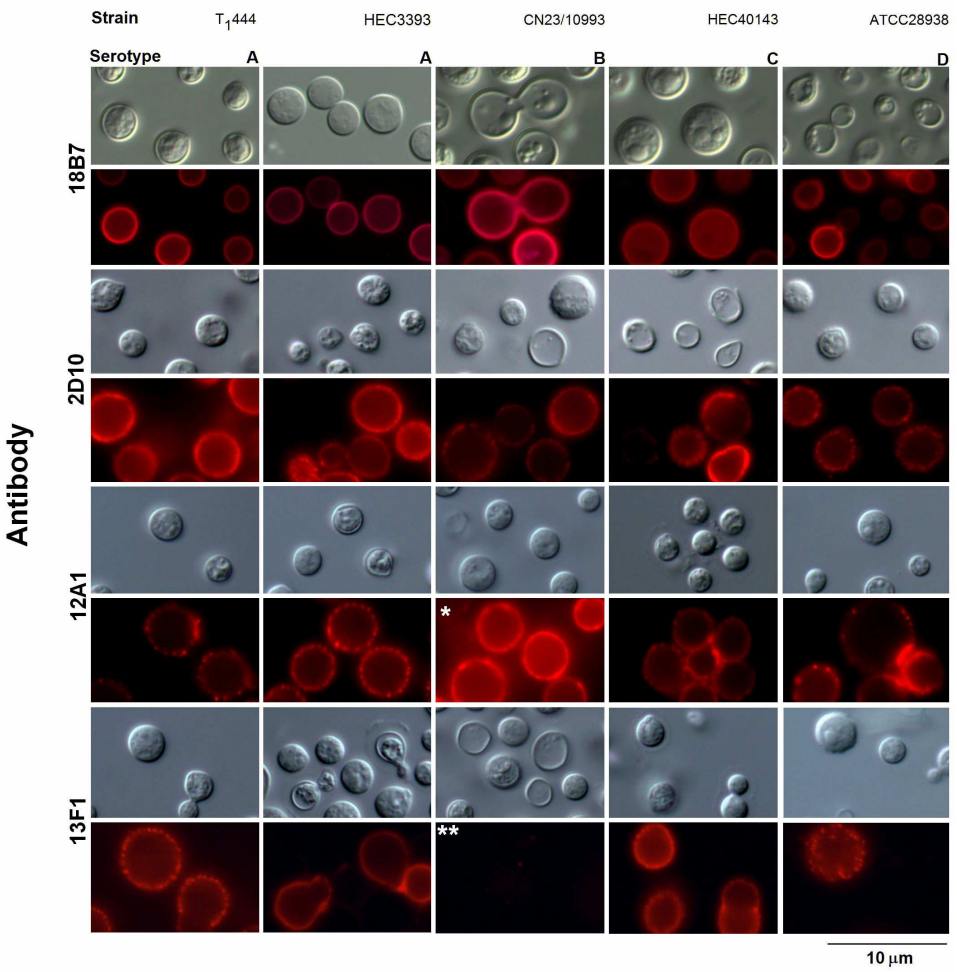


565

566 **Figure 5. Reactivity of *C. neoformans* and *C. gattii* isolates with four monoclonal**
567 **antibodies to GXM.** Fungal strains and serotypes are indicated on the top panels;
568 antibodies are shown on the left. Differential interferential contrast (gray) and
569 fluorescence (red) images are shown. Overreaction of CN23/10993 cells with
570 antibody 12A1 (single asterisk) and lack of reactivity with antibody 13F1 (double
571 asterisks) are highlighted.

572

573

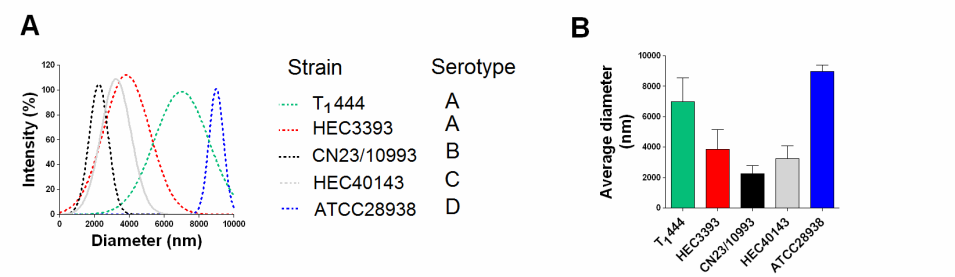


574

575

576 **Figure 6. Diameter of GXM fractions of different isolates of *C. neoformans* and**

577 ***C. gattii*.** Effective diameter distribution of GXM (A) and related average values (B)

578 are shown. Serotypes are indicated for each strain.

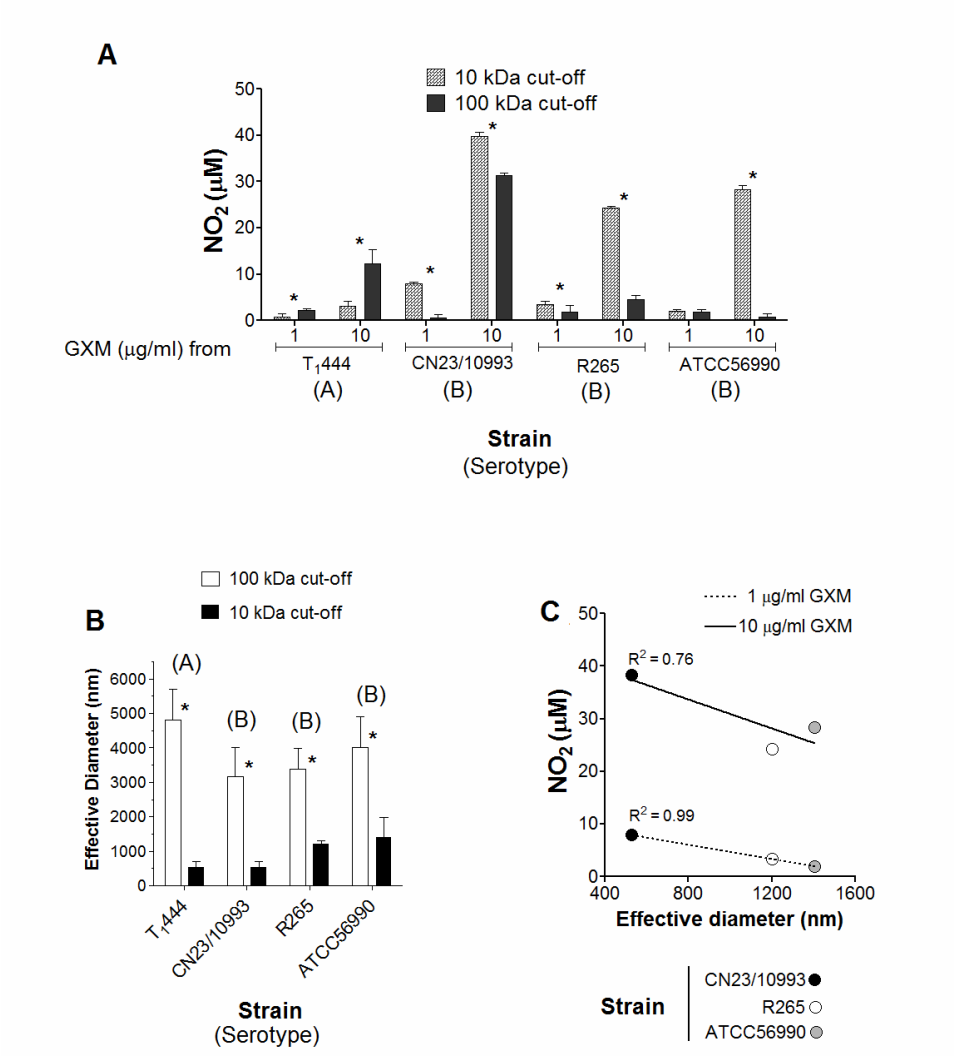


**Figure 7**. **NO induction by GXM fractions of different molecular masses and effective diameters.** A. Stimulation of macrophage-like cells with the GXM fractions results in differential production of NO. Asterisks denote significant differences after stimulation of phagocytes with GXM fractions ($P$<0.0001). B. Effective diameter determination of fractions obtained by sequential ultrafiltration through 100 kDa and 10 kDa cut-off filtration discs. Asterisks denote statistical significance after comparison of the differences in effective diameter ($P$<0.0001). C. Correlation

analysis of effective diameter of serotype B GXM samples in the 10-100 kDa range and their ability to induce NO. Serotypes are indicated for each strain.

589 **Table 1. Electronegativity of polysaccharides from five different strains of**

590 ***C. neoformans* and *C. gattii*.**

591

| Strain | Serotype | Zeta Potential (mV) | Mobility (μ/s)/(V/cm) |
|---|---|---|---|
| $T_1$444 | A | -34.50 ±0.32 | -2.70±0.02 |
| HEC3393 | A | -33.36±0.51 | -2.61±0.04 |
| CN23/10993 | B | -33.34±0.21 | -2.60±0.02 |
| HEC40143 | C | -38.15±0.41 | -2.98±0.03 |
| ATCC28938 | D | -34.62±0.45 | -2.71±0.04 |

592

## References


1. **Bicanic, T., and T. S. Harrison**. 2004. Cryptococcal meningitis. Br Med Bull **72**:99-118.
2. **Biondo, C., A. Midiri, L. Messina, F. Tomasello, G. Garufi, M. R. Catania, M. Bombaci, C. Beninati, G. Teti, and G. Mancuso**. 2005. MyD88 and TLR2, but not TLR4, are required for host defense against Cryptococcus neoformans. Eur J Immunol **35**:870-878.
3. **Casadevall, A., W. Cleare, M. Feldmesser, A. Glatman-Freedman, D. L. Goldman, T. R. Kozel, N. Lendvai, J. Mukherjee, L. A. Pirofski, J. Rivera, A. L. Rosas, M. D. Scharff, P. Valadon, K. Westin, and Z. Zhong**. 1998. Characterization of a murine monoclonal antibody to Cryptococcus neoformans polysaccharide that is a candidate for human therapeutic studies. Antimicrob Agents Chemother **42**:1437-1446.
4. **Casadevall, A., J. Mukherjee, and M. D. Scharff**. 1992. Monoclonal antibody based ELISAs for cryptococcal polysaccharide. J Immunol Methods **154**:27-35.
5. **Chiapello, L. S., J. L. Baronetti, A. P. Garro, M. F. Spesso, and D. T. Masih**. 2008. Cryptococcus neoformans glucuronoxylomannan induces macrophage apoptosis mediated by nitric oxide in a caspase-independent pathway. Int Immunol **20**:1527-1541.
6. **Collopy-Junior, I., F. F. Esteves, L. Nimrichter, M. L. Rodrigues, C. S. Alviano, and J. R. Meyer-Fernandes**. 2006. An ectophosphatase activity in Cryptococcus neoformans. FEMS yeast research **6**:1010-1017.
7. **Da Silva, C. A., D. Hartl, W. Liu, C. G. Lee, and J. A. Elias**. 2008. TLR-2 and IL-17A in chitin-induced macrophage activation and acute inflammation. J Immunol **181**:4279-4286.
8. **De Jesus, M., S. K. Chow, R. J. Cordero, S. Frases, and A. Casadevall**. Galactoxylomannans from Cryptococcus neoformans varieties neoformans and grubii are structurally and antigenically variable. Eukaryotic cell.
9. **Doering, T. L.** 2000. How does Cryptococcus get its coat? Trends in microbiology **8**:547-553.
10. **Fonseca, F. L., S. Frases, A. Casadevall, O. Fischman-Gompertz, L. Nimrichter, and M. L. Rodrigues**. 2009. Structural and functional properties of the Trichosporon asahii glucuronoxylomannan. Fungal Genet Biol **46**:496-505.
11. **Frases, S., L. Nimrichter, N. B. Viana, A. Nakouzi, and A. Casadevall**. 2008. Cryptococcus neoformans capsular polysaccharide and exopolysaccharide fractions manifest physical, chemical, and antigenic differences. Eukaryotic cell **7**:319-327.
12. **Frases, S., B. Pontes, L. Nimrichter, N. B. Viana, M. L. Rodrigues, and A. Casadevall**. 2009. Capsule of Cryptococcus neoformans grows by enlargement of polysaccharide molecules. Proceedings of the National Academy of Sciences of the United States of America **106**:1228-1233.
13. **Garcia-Rivera, J., Y. C. Chang, K. J. Kwon-Chung, and A. Casadevall**. 2004. Cryptococcus neoformans CAP59 (or Cap59p) is involved in the extracellular trafficking of capsular glucuronoxylomannan. Eukaryotic cell **3**:385-392.
14. **Gautam, J. K., Ashish, L. D. Comeau, J. K. Krueger, and M. F. Smith, Jr.** 2006. Structural and functional evidence for the role of the TLR2 DD loop in TLR1/TLR2 heterodimerization and signaling. The Journal of biological chemistry **281**:30132-30142.

15. **Green, L. C., D. A. Wagner, J. Glogowski, P. L. Skipper, J. S. Wishnok, and S. R. Tannenbaum**. 1982. Analysis of nitrate, nitrite, and [15N]nitrate in biological fluids. Anal Biochem **126**:131-138.
16. **Hajjar, A. M., D. S. O'Mahony, A. Ozinsky, D. M. Underhill, A. Aderem, S. J. Klebanoff, and C. B. Wilson**. 2001. Cutting edge: functional interactions between toll-like receptor (TLR) 2 and TLR1 or TLR6 in response to phenol-soluble modulin. J Immunol **166**:15-19.
17. **Jin, M. S., S. E. Kim, J. Y. Heo, M. E. Lee, H. M. Kim, S. G. Paik, H. Lee, and J. O. Lee**. 2007. Crystal structure of the TLR1-TLR2 heterodimer induced by binding of a tri-acylated lipopeptide. Cell **130**:1071-1082.
18. **Jin, M. S., and J. O. Lee**. 2008. Structures of the toll-like receptor family and its ligand complexes. Immunity **29**:182-191.
19. **Kidd, S. E., F. Hagen, R. L. Tscharke, M. Huynh, K. H. Bartlett, M. Fyfe, L. Macdougall, T. Boekhout, K. J. Kwon-Chung, and W. Meyer**. 2004. A rare genotype of Cryptococcus gattii caused the cryptococcosis outbreak on Vancouver Island (British Columbia, Canada). Proceedings of the National Academy of Sciences of the United States of America **101**:17258-17263.
20. **Kozel, T. R., S. M. Levitz, F. Dromer, M. A. Gates, P. Thorkildson, and G. Janbon**. 2003. Antigenic and biological characteristics of mutant strains of Cryptococcus neoformans lacking capsular O acetylation or xylosyl side chains. Infection and immunity **71**:2868-2875.
21. **Krishnegowda, G., A. M. Hajjar, J. Zhu, E. J. Douglass, S. Uematsu, S. Akira, A. S. Woods, and D. C. Gowda**. 2005. Induction of proinflammatory responses in macrophages by the glycosylphosphatidylinositols of Plasmodium falciparum: cell signaling receptors, glycosylphosphatidylinositol (GPI) structural requirement, and regulation of GPI activity. J Biol Chem **280**:8606-8616.
22. **Kumar, H., T. Kawai, and S. Akira**. 2009. Toll-like receptors and innate immunity. Biochem Biophys Res Commun **388**:621-625.
23. **Kwon-Chung, K. J., and A. Varma**. 2006. Do major species concepts support one, two or more species within Cryptococcus neoformans? FEMS yeast research **6**:574-587.
24. **Larsen, R. A., P. G. Pappas, J. Perfect, J. A. Aberg, A. Casadevall, G. A. Cloud, R. James, S. Filler, and W. E. Dismukes**. 2005. Phase I evaluation of the safety and pharmacokinetics of murine-derived anticryptococcal antibody 18B7 in subjects with treated cryptococcal meningitis. Antimicrob Agents Chemother **49**:952-958.
25. **Lee, C. G.** 2009. Chitin, chitinases and chitinase-like proteins in allergic inflammation and tissue remodeling. Yonsei Med J **50**:22-30.
26. **Lee, C. G., C. A. Da Silva, J. Y. Lee, D. Hartl, and J. A. Elias**. 2008. Chitin regulation of immune responses: an old molecule with new roles. Curr Opin Immunol **20**:684-689.
27. **Levitz, S. M.** 2002. Receptor-mediated recognition of Cryptococcus neoformans. Nippon Ishinkin Gakkai Zasshi **43**:133-136.
28. **Levitz, S. M.** 2004. Interactions of Toll-like receptors with fungi. Microbes and infection / Institut Pasteur **6**:1351-1355.
29. **Liang, S., K. B. Hosur, S. Lu, H. F. Nawar, B. R. Weber, R. I. Tapping, T. D. Connell, and G. Hajishengallis**. 2009. Mapping of a microbial protein domain involved in binding and activation of the TLR2/TLR1 heterodimer. J Immunol **182**:2978-2985.

30. **McClelland, E. E., P. Bernhardt, and A. Casadevall**. 2005. Coping with multiple virulence factors: which is most important? PLoS pathogens **1**:e40.
31. **McFadden, D., O. Zaragoza, and A. Casadevall**. 2006. The capsular dynamics of Cryptococcus neoformans. Trends in microbiology **14**:497-505.
32. **Merkle, R. K., and I. Poppe**. 1994. Carbohydrate composition analysis of glycoconjugates by gas-liquid chromatography/mass spectrometry. Methods in enzymology **230**:1-15.
33. **Mitchell, D. H., T. C. Sorrell, A. M. Allworth, C. H. Heath, A. R. McGregor, K. Papanaoum, M. J. Richards, and T. Gottlieb**. 1995. Cryptococcal disease of the CNS in immunocompetent hosts: influence of cryptococcal variety on clinical manifestations and outcome. Clin Infect Dis **20**:611-616.
34. **Monari, C., F. Bistoni, A. Casadevall, E. Pericolini, D. Pietrella, T. R. Kozel, and A. Vecchiarelli**. 2005. Glucuronoxylomannan, a microbial compound, regulates expression of costimulatory molecules and production of cytokines in macrophages. J Infect Dis **191**:127-137.
35. **Monari, C., F. Bistoni, and A. Vecchiarelli**. 2006. Glucuronoxylomannan exhibits potent immunosuppressive properties. FEMS yeast research **6**:537-542.
36. **Monari, C., E. Pericolini, G. Bistoni, A. Casadevall, T. R. Kozel, and A. Vecchiarelli**. 2005. Cryptococcus neoformans capsular glucuronoxylomannan induces expression of fas ligand in macrophages. J Immunol **174**:3461-3468.
37. **Mukherjee, J., G. Nussbaum, M. D. Scharff, and A. Casadevall**. 1995. Protective and nonprotective monoclonal antibodies to Cryptococcus neoformans originating from one B cell. The Journal of experimental medicine **181**:405-409.
38. **Mukherjee, J., M. D. Scharff, and A. Casadevall**. 1992. Protective murine monoclonal antibodies to Cryptococcus neoformans. Infection and immunity **60**:4534-4541.
39. **Nakamura, K., K. Miyagi, Y. Koguchi, Y. Kinjo, K. Uezu, T. Kinjo, M. Akamine, J. Fujita, I. Kawamura, M. Mitsuyama, Y. Adachi, N. Ohno, K. Takeda, S. Akira, A. Miyazato, M. Kaku, and K. Kawakami**. 2006. Limited contribution of Toll-like receptor 2 and 4 to the host response to a fungal infectious pathogen, Cryptococcus neoformans. FEMS Immunol Med Microbiol **47**:148-154.
40. **Nimrichter, L., S. Frases, L. P. Cinelli, N. B. Viana, A. Nakouzi, L. R. Travassos, A. Casadevall, and M. L. Rodrigues**. 2007. Self-aggregation of Cryptococcus neoformans capsular glucuronoxylomannan is dependent on divalent cations. Eukaryotic cell **6**:1400-1410.
41. **Nosanchuk, J. D., and A. Casadevall**. 1997. Cellular charge of Cryptococcus neoformans: contributions from the capsular polysaccharide, melanin, and monoclonal antibody binding. Infection and immunity **65**:1836-1841.
42. **Nussbaum, G., W. Cleare, A. Casadevall, M. D. Scharff, and P. Valadon**. 1997. Epitope location in the Cryptococcus neoformans capsule is a determinant of antibody efficacy. The Journal of experimental medicine **185**:685-694.
43. **Perfect, J. R., and A. Casadevall**. 2002. Cryptococcosis. Infectious disease clinics of North America **16**:837-874, v-vi.
44. **Roeder, A., C. J. Kirschning, R. A. Rupec, M. Schaller, and H. C. Korting**. 2004. Toll-like receptors and innate antifungal responses. Trends in microbiology **12**:44-49.
45. **Schindler, U., and V. R. Baichwal**. 1994. Three NF-kappa B binding sites in the human E-selectin gene required for maximal tumor necrosis factor alpha-induced expression. Mol Cell Biol **14**:5820-5831.

46. **Shoham, S., C. Huang, J. M. Chen, D. T. Golenbock, and S. M. Levitz**. 2001. Toll-like receptor 4 mediates intracellular signaling without TNF-alpha release in response to Cryptococcus neoformans polysaccharide capsule. J Immunol **166**:4620-4626.

47. **Sorgi, C. A., A. Secatto, C. Fontanari, W. M. Turato, C. Belanger, A. I. de Medeiros, S. Kashima, S. Marleau, D. T. Covas, P. T. Bozza, and L. H. Faccioli**. 2009. Histoplasma capsulatum cell wall {beta}-glucan induces lipid body formation through CD18, TLR2, and dectin-1 receptors: correlation with leukotriene B4 generation and role in HIV-1 infection. J Immunol **182**:4025-4035.

48. **Speed, B., and D. Dunt**. 1995. Clinical and host differences between infections with the two varieties of Cryptococcus neoformans. Clin Infect Dis **21**:28-34; discussion 35-26.

49. **Sweetser, M. T., T. Hoey, Y. L. Sun, W. M. Weaver, G. A. Price, and C. B. Wilson**. 1998. The roles of nuclear factor of activated T cells and ying-yang 1 in activation-induced expression of the interferon-gamma promoter in T cells. J Biol Chem **273**:34775-34783.

50. **Triantafilou, M., F. G. Gamper, R. M. Haston, M. A. Mouratis, S. Morath, T. Hartung, and K. Triantafilou**. 2006. Membrane sorting of toll-like receptor (TLR)-2/6 and TLR2/1 heterodimers at the cell surface determines heterotypic associations with CD36 and intracellular targeting. The Journal of biological chemistry **281**:31002-31011.

51. **Vecchiarelli, A.** 2007. Fungal capsular polysaccharide and T-cell suppression: the hidden nature of poor immunogenicity. Crit Rev Immunol **27**:547-557.

52. **Yauch, L. E., M. K. Mansour, and S. M. Levitz**. 2005. Receptor-mediated clearance of Cryptococcus neoformans capsular polysaccharide in vivo. Infection and immunity **73**:8429-8432.

53. **Yauch, L. E., M. K. Mansour, S. Shoham, J. B. Rottman, and S. M. Levitz**. 2004. Involvement of CD14, toll-like receptors 2 and 4, and MyD88 in the host response to the fungal pathogen Cryptococcus neoformans in vivo. Infection and immunity **72**:5373-5382.

54. **Zaragoza, O., M. L. Rodrigues, M. De Jesus, S. Frases, E. Dadachova, and A. Casadevall**. 2009. The capsule of the fungal pathogen Cryptococcus neoformans. Adv Appl Microbiol **68**:133-216.